Dynein Light Chain LC8 Promotes Assembly of the Coiled-Coil Domain of Swallow Protein†

Lei Wang,‡ Michael Hare,§ Thomas S. Hays,|| and Elisar Barbar*,‡,§

Department of Biological Sciences, Ohio University, Athens, Ohio 45701, Department of Biochemistry and Biophysics, Oregon State University, Corvallis, Oregon 97331, and Department of Genetics, Cell Biology, and Development, University of Minnesota, Minneapolis, Minnesota 55455

Received December 29, 2003; Revised Manuscript Received February 6, 2004

ABSTRACT: LC8 is a highly conserved light-chain subunit of cytoplasmic dynein that is thought to play a fundamental role in both the assembly of the motor complex and the recruitment of cargo. An interaction between LC8 and the *Drosophila* protein swallow has been previously characterized and supports a role for dynein in the localization of maternal morphogens during oogenesis. Swallow is required for the proper localization of *bicoid* mRNA, the anterior determinant that plays a critical role in establishment of the *Drosophila* embryonic axis. In this work, we prepared constructs of swallow, each containing a predicted coiled-coil domain and variable surrounding segments that lie within the domain proposed to interact with LC8. The interaction between LC8 and swallow domains was characterized by glutathione S-transferase (GST) pull-down assays, limited proteolysis followed by mass spectrometry, and circular dichroic spectroscopy. Hydrodynamic measurements, covalent cross-linking, and circular dichroic spectroscopy show that this domain of swallow is an unstable dimeric coiled-coil. Upon LC8 binding, however, the coiled-coil becomes significantly more stable. A possible general role for LC8 in macromolecular assembly is discussed.

LC8[1] was first identified as a constituent of axonemal dynein from the outer arm of *Chlamydomonas* flagella (*1*). Since then, several highly homologous cytoplasmic forms were found by molecular cloning and GenBank database searches (*2*). High evolutionary conservation (94% homology between *Drosophila* and human) and other evidence indicate that LC8 fulfills several distinct and essential roles in the cell (*3*−*5*). Molecular genetic studies in *Drosophila* show that null mutations are lethal, while hypomorphic mutations in a *Drosophila* LC8 gene result in oogenesis defects and female sterility (*3*, *6*). The importance of LC8 in oogenesis and female sterility is consistent with cytoplasmic dynein heavy-chain function in oocyte determination and development (*7*). The LC8 light chain is presumed to have a fundamental role in the assembly of the dynein complex since it is a stoichiometric component of a tight subcomplex located at the dynein base (*8*) and is utilized by both flagellar and cytoplasmic dynein motors. There is evidence that LC8 acts in a similar manner to facilitate the assembly of the actin-based motor myosin V (*9*, *10*). In addition, numerous reports of interactions with diverse cellular proteins indicate that LC8 may have functions unrelated to dynein (*11*−*18*). For example, LC8 is known to suppress the activity of the nuclear transcription factor TRPS1 (*11*). These various interactions have suggested a role for LC8 as a potential adapter protein or "molecular glue" that mediates the interactions of proteins within multiprotein complexes (*15*).

In *Drosophila*, LC8 was found to interact with a protein called swallow, a gene product required for the proper localization of *bicoid* mRNA (*13*, *19*). During *Drosophila* development, localization of *bicoid* RNA at the anterior pole of the oocyte is necessary to specify the anterior−posterior axis of the embryo (*20*). An interaction between LC8 and the swallow protein deduced from yeast two-hybrid assays and coimmunoprecipitation studies indicate that LC8 may link dynein with the *bicoid* mRNA-containing complex (*13*). The linkage between swallow and the LC8 light chain has suggested that dynein mediates either microtubule-based transport or a tethering of *bicoid* mRNA to the anterior pole of the *Drosophila* oocyte. The yeast two-hybrid assays identified a predicted coiled-coil domain of swallow, residues 197−295, as required for the interaction with LC8. In the present work, we provide additional evidence for a direct interaction between LC8 and swallow constructs by using GST pull-down assays. Significantly, structural characterization of both free and bound swallow protein reveals considerable differences in conformation and stability that are induced upon binding to LC8. Our results support a role

† This work is supported by NSF Career Grant MCB-0238094 and NIH GM60969 (E.B.) and NIH GM053695 (T.S.H.).

* Corresponding author: tel 541-737-4143; fax 541-737-0481; e-mail barbare@science.oregonstate.edu.

‡ Ohio University.

§ Oregon State University.

|| University of Minnesota.

[1] Abbreviations: LC8, 10 kDa dynein light chain (also referred to as PIN, DLC1, or DLC8); IC74, 74 kDa dynein intermediate chain; $Swa^{191-297}$, $Swa^{206-297}$, and $Swa^{206-283}$, constructs of *Drosophila* swallow protein that include amino acids 191−297, 206−297, and 206−283, respectively; GST, glutathione S-transferase; ESI-MS, electrospray ionization mass spectrometry; CD, circular dichroism; TCEP, tris(2-carboxyethyl)phosphine hydrochloride; PCR, polymerase chain reaction; EDTA, ethylenediaminetetraacetic acid; PMSF, phenylmethanesulfonyl fluoride; SDS, sodium dodecyl sulfate; PAGE, polyacrylamide gel electrophoresis.

10.1021/bi036328x CCC: $27.50
Published on Web 03/23/2004

for LC8 that includes inducing folding and/or oligomerization of its binding partners in the process of forming a cargo docking site.

MATERIALS AND METHODS

Cloning. Several constructs of *Drosophila* swallow protein (GenBank Accession Number CAA39500) were made: $Swa^{191-297}$, $Swa^{206-297}$, and $Swa^{206-283}$ correspond to amino acids 191−297, 206−297, and 206−283, respectively. The fragments of *swallow* cDNA were amplified by PCR, cloned into PCRII-TOPO vector by use of a TOPO TA cloning kit (Invitrogen), subcloned into pET15d vector, which has an N-terminal hexa-His tag (Novagen), or pGEX-6p-3 vector (Pharmacia Biotech), and then transformed into *Escherichia coli* BL21(DE3) or BL21 host cells for expression. All constructs were verified by automated sequencing.

Protein Expression and Purification. The BL21(DE3) host cells transformed with the pET15d-*swallow* plasmid were grown in LB medium at 37 °C to A_{600} of ∼0.6 before induction with 0.4 mM of isopropyl β-D-galactopyranoside for 3.5 h at 25 °C with vigorous shaking. The cells were harvested and resuspended in lysis buffer containing 50 mM sodium phosphate buffer, 500 mM NaCl, 2 mM PMSF, 5 mM benzamidine, and 10 mM β-mercaptoethanol, pH 6.0. After sonication and centrifugation at 18000*g* for 30 min, the crude extract was purified by affinity chromatography on a Ni^{2+}-nitrilotriacetic acid affinity column (Ni−NTA, Qiagen) by elution with 350 mM imidazole, followed by extensive dialysis in a buffer containing 50 mM sodium phosphate, 0.5 M NaCl, 10−20 mM β-mercaptoethanol, and 5−10% glycerol, pH 6.0. The polyhistidine fusion peptide resulted in the addition of 17 residues N-terminal to the swallow constructs sequence. The expression and purification of LC8 was described previously (*21*, *22*). The identities of all proteins were confirmed by mass spectrometry. For performing GST pull-down assays, GST-fused swallow constructs were overexpressed in strain BL21 and purified on GSH−Sepharose 4B affinity columns (Amersham Biosciences) following the protocol provided by the manufacturer.

GST Pull-Down Assays. All the recombinant protein samples were dialyzed in phosphate-buffered saline, PBS (140 mM NaCl, 2.7 mM KCl, 10 mM Na_2HPO_4, and 1.8 mM KH_2PO_4, pH 7.5), supplemented with 1 mM EDTA, and 5 mM β-mercaptoethanol. A 10 μL bed volume of glutathione−Sepharose resin was added to 80 μg of GST-$Swa^{191-297}$, and the mixture was incubated on ice for 30 min before addition of purified LC8 at 1:1 molar ratio. The mixture was incubated on ice for another 1−3 h. The resin was then washed 4 times with 500 μL of buffer. The bound protein was eluted from the resin with 30 μL of 2× SDS sample buffer (117 mM Tris-HCl, pH 6.8, 3.4% SDS, 12% glycerol, 1.7% β-mercaptoethanol, and 0.04% bromophenol blue) and boiled for 5 min. After centrifugation, the supernatant was subjected to SDS−15% PAGE followed by staining with Coomassie brilliant blue-G250.

Protein Cross-Linking. Two distinct types of protein cross-linkers, BS^3 [bis(sulfosuccinimido) suberate, Pierce] and bBBr (dibromobimane, Molecular Probes) were used. BS^3 is a primary amine-reactive bifunctional N-hydroxysuccinimide ester that cross-links the ε-amine of lysine with a spacer arm length of 11.4 Å. A stock solution of 40 mM BS^3 in DMSO was added directly to 5 μM $Swa^{191-297}$ in 50 mM sodium phosphate, 500 mM NaCl, 10 mM β-mercaptoethanol, and 5% glycerol, pH 6.0, to final concentrations of 60, 125, 250, and 500 μM. After incubating at 25 °C for 1 h, reactions were terminated by addition of sample loading buffer with β-mercaptoethanol and visualized by SDS−15% PAGE followed by Coomassie brilliant blue staining. A stock solution of 24 mM bBBr, a zero-length thiol-specific cross-linker, was added directly to 50 μM $Swa^{206-283}$ in 50 mM sodium phosphate, 500 mM NaCl, and 2 mM β-mercaptoethanol, pH 6.5, to final concentrations of 25, 50, 100, 250, and 500 μM. The reactions were carried out at 25 °C for 2 h. For the temperature dependence experiments, 5 μM of $Swa^{191-297}$ in 50 mM sodium phosphate, 200 mM NaCl, and 1 mM TCEP, pH 6.5, were preincubated with equal concentrations of LC8 or equal volumes of buffer for 1 h at 30 or 4 °C before addition of bBBr to a final concentration of 200 μM. The reactions were carried out either at 30 °C for 2 h or at 4 °C overnight.

Limited Proteolysis and Electrospray Ionization Mass Spectrometry. $Swa^{191-297}$ was mixed with LC8 at approximately 1:1 molar ratio and incubated on ice for at least 2 h before digestion. For control experiments, equal volumes of buffer were added instead of LC8. Sequencing-grade trypsin (Promega) was used at an enzyme-to-substrate ratio of 1:50 (w/w). Proteolysis was performed at 25 °C for up to 2 h. Aliquots of 50 μL were taken at increasing time intervals and the reactions were quenched by addition of PMSF to a final concentration of 4 mM. For each time interval, 10 μL of the sample was subjected to SDS−PAGE followed by Coomassie brilliant blue staining and the rest was analyzed by ESI-MS on a Bruker Esquire system with Bruker Data Analysis 2 software.

Circular Dichroism Spectroscopy. CD spectra were obtained on a Jasco 715 spectropolarimeter equipped with a Peltier thermoelectric temperature controller (model PFD-335S), which permits accurate temperature control. A built-in magnetic stirrer allows for rapid equilibration within the cell. Samples for CD measurements were prepared in 50 mM potassium phosphate buffer containing 600 mM KCl and 2 mM β-mercaptoethanol, pH 6.0, or in 10 mM sodium phosphate buffer with 100 mM NaCl and 2 mM β-mercaptoethanol for thermal unfolding experiments. Thermal unfolding was measured by monitoring the CD signal at 222 nm in a 1 cm cuvette with constant stirring, allowing 4 min of equilibration per 3 °C temperature increment. Temperature was dropped to 25 °C after 40 and 65 °C to check the reversibility of each transition. Protein concentrations were determined spectrophotometrically and by densitometric analysis of Coomassie-stained SDS−polyacrylamide gel and comparison with protein standards of known concentrations.

The helical content, f_H, was estimated from the mean residue ellipticity, θ_H, measured at 222 nm by use of (*23*)

$$f_H = (\theta_{222} - \theta_C)/(\theta_H - \theta_C)$$

where $\theta_H = (250T - 44\,000)(1 - 3/n)$, $\theta_C = 2220 - 53T$, n is the number of residues, and T is temperature in Kelvin.

Size-Exclusion Chromatography. A Superdex 75 HR analytical column (Amersham Biosciences) was equilibrated with 50 mM sodium phosphate, 0.4 M sodium sulfate, and

5 mM β-mercaptoethanol, pH 6.0. Approximately 1 mL of Swa $^{206-283}$ was applied at a flow rate of 0.2 mL/min at room temperature. The globular protein molecular mass standards of 220, 65, 45, 24, and 12 kDa (Sigma) were eluted under the same conditions. Samples were monitored by UV absorption at both 220 and 280 nm.

Sedimentation Velocity Ultracentrifugation. Sedimentation velocity data were collected on a Beckman XL1 analytical ultracentrifuge at a speed of 50 000 rpm at 20 °C for 8 h. Samples were placed into double-sector interference cells with sample buffer as a reference. Data were processed and analyzed with the Sedanal software v2.91 developed by Stafford (*24*). For apparent molecular weight determination, the data were analyzed by the time-derivative method with the d*c*/d*t* function, and for the dissociation constant, preprocessed data were analyzed with the fit preprocessed data function of the software.

Structure Prediction. The Coil program (*25*) was used to predict residues in the coiled-coil conformation and Multicoil (*26*) to determine the probability of the coiled-coil to be dimeric or trimeric. The secondary structure was predicted with PSIPRED (*27*).

RESULTS

Design of Recombinant Swallow Constructs. Yeast two-hybrid screening of swallow fragments determined that residues 197−295 are sufficient for strong interaction with dynein light-chain LC8 (*13*). Within this segment, sequence analysis predicts that residues 206−275 are an α-helical coiled-coil, and residues 276−295 are primarily unstructured. The sequence KATQT, which is found in many LC8 binding partners and may act as an LC8 recognition sequence (*28*), occurs in the predicted unstructured segment. A diagram of the native sequence of swallow, a 548 amino acid protein, and the three constructs prepared in this work is shown in Figure 1A. Swa$^{191-297}$ includes the segment mapped by yeast two-hybrid assay with a few extra flanking residues. The resultant expressed protein is poorly soluble and precipitates at concentrations higher than 0.2 mg/mL. Swa$^{206-297}$ lacks the residues that are N-terminal to the predicted coiled-coil and is poorly soluble. Both GST and His-tagged forms of these constructs have limited solubility. Swa$^{206-283}$ contains the predicted coiled-coil but lacks the 14 amino acids containing the KATQT sequence at the C-terminal end and is highly soluble. In experiments that require high protein concentration, Swa$^{206-283}$ was used. As described below, Swa$^{206-283}$ differs from the other two constructs only in its lack of binding to LC8, while Swa$^{206-297}$ and Swa$^{191-297}$ show similar behavior in all experiments.

Circular Dichroic Characterization of Swallow Constructs. Figure 1B illustrates a helical wheel diagram of the segment predicted to be coiled-coil. In agreement with structure prediction, the CD spectrum of Swa$^{206-283}$ shows double minima at 208 and 222 nm, typical for α-helical conformation (Figure 2A). At 5 °C, the calculated helical content is approximately 71%, corresponding to 70 out of 99 residues in α-helical conformation (10 heptad repeats). At 23 °C, the helical content decreases to 66%. The $[\theta_{222}]/[\theta_{208}]$ ratios for Swa$^{206-283}$ at 23 and 5 °C are 1.06 and 1.10, respectively. A ratio close to 1 and higher indicates the existence of supercoiling (*29*−*31*). At 40 °C, the helical content decreases

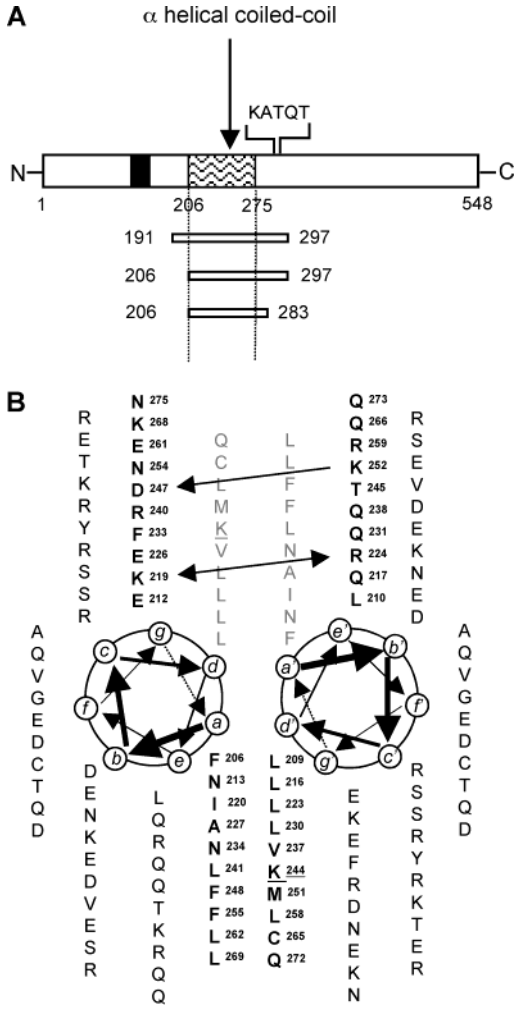

FIGURE 1: (A) Diagram of full-length *Drosophila* swallow protein and various constructs used in this work. *Drosophila* swallow is a 548 amino acid protein that contains a predicted α-helical coiled-coil at 206−275 followed by the sequence KATQT (291−295), which is present in almost all LC8 binding partners. The black bar corresponds to the putative RNA recognition motif. The 197−295 segment is necessary for LC8 binding, as shown by yeast two-hybrid assays (*13*). Constructs of swallow are represented by numbered bars denoting their sequence positions. (B) Hypothetical helical wheel representation of residues 206−275. Positions in the heptad repeats are denoted by a−g. The putative g (i) → e′ (i + 5) interactions are shown by arrows. The double-headed arrow indicates the potential repulsive force between K219 and R224. Attractive electrostatic interaction between D247 and K252 is depicted by an arrow pointing to D247. A charged residue at the coiled-coil interface is underlined.

to 38% and the $[\theta_{222}]/[\theta_{208}]$ ratio becomes 0.84, which is typical of a helical conformation without supercoiling. At 65 °C, the protein is unfolded as indicated by helical content of 13% and a wavelength shift from 208 to 203 nm. The reversibility of supercoiling is shown by the reproducibility of spectra at 5 °C before (●) and after (○) the temperature is raised to 40 °C. After 65 °C, reversibility of unfolding is about 95% (data not shown). CD spectra and thermal denaturation curves of Swa$^{206-297}$ and Swa$^{191-297}$ are similar (data not shown), indicating that their stability is determined primarily by the coiled-coil segment common to them.

The thermal denaturation curve of Swa$^{206-283}$ at 12 μM protein concentration monitored at 222 nm was determined in the temperature range of 5−75 °C and shows an apparent three-state unfolding with the midpoint of the first transition

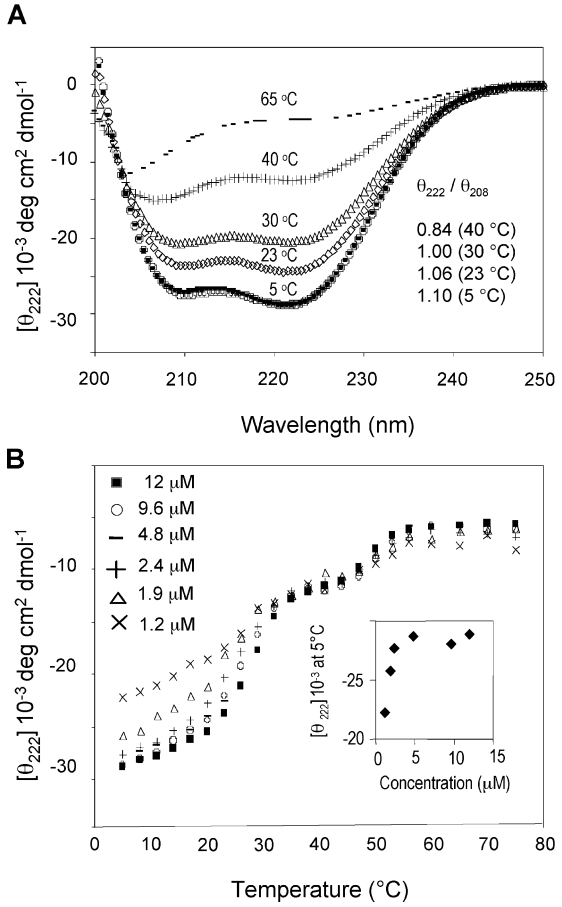

FIGURE 2: Thermal unfolding of Swa$^{206-283}$ monitored by CD. (A) CD spectra were acquired for Swa$^{206-283}$ at 5, 23, 30, 40, and 65 °C. The protein concentration used was 8.4 μM in 50 mM potassium phosphate, 0.6 M KCl, and 2 mM β-mercaptoethanol, pH 6.0. The temperature was dropped to 5 °C after heating to 40 °C to check for reversibility of supercoiling (○). (B) Thermal unfolding of Swa$^{206-283}$ monitored at [θ_{222}] at increasing protein concentration. The protein concentrations used were 1.2, 1.9, 2.4, 4.8, and 12 μM in 10 mM sodium phosphate, 0.1 M NaCl, and 2 mM β-mercaptoethanol or in 1 mM TCEP, pH 6.0. The inset is a plot of molar ellipticity at 222 nm at 5 °C versus Swa$^{206-283}$ concentration. At concentrations higher than 4.8 μM, Swa$^{206-283}$ is primarily dimeric.

at 24 °C and the midpoint of the second transition at 50 °C (Figure 2B, ■). Thermal denaturation curves in the protein concentration range of 1.2−12 μM show that the first transition is concentration-dependent and hence arises primarily from changes in intermolecular interactions, while the second transition is not concentration-dependent and arises primarily from changes in intramolecular interactions. The protein concentration dependence of the negative mean residue ellipticity at 222 nm at 5 °C suggests an increase in the population of the folded coiled-coil before it reaches saturation at >4.8 μM (Figure 2B, inset).

Association State(s) of Swallow Constructs. Sequence analysis by use of the MultiCoil program predicts that Swa$^{191-297}$ has a higher propensity to form a two-stranded rather than a three-stranded coiled-coil. To determine its oligomerization state, we performed chemical cross-linking experiments. Since there are numerous lysine residues in Swa$^{191-297}$, BS^3, which cross-links two ϵ-amines of lysine closer than 11.4 Å, was used. Bands appearing at 29 kDa (Figure 3A) indicate that Swa$^{191-297}$ is a dimer (monomer mass of 13.5 kDa). Successful cross-linking of Swa$^{206-283}$ with bBBr, a zero-length thiol cross-linker (Figure 3B), indicates that a cysteine residue, presumably Cys265, is at the interface and cross-links with Cys265′, consistent with the helical-wheel diagram (Figure 1B). These results show that the predicted coiled-coil domain of swallow is dimeric, with a cysteine residue located at the interface and a lysine residue close to the interface.

To characterize the hydrodynamic behavior of this domain, we performed size-exclusion chromatography on Swa$^{206-283}$ at protein concentrations of 4 and 40 μM. Since Swa$^{206-283}$ and Swa$^{191-297}$ show similar cross-linking behavior (Figure 3 and data not shown), Swa$^{206-283}$ was used here to attain the higher concentrations needed for this experiment. Swa$^{206-283}$ elutes as two peaks (** and *), indicating the existence of two molecular states in slow exchange (Figure 4). The proportion of the low molecular weight population (*) is higher at 4 μM than at 40 μM, indicating that the equilibrium shifts toward the low molecular weight state at low protein concentration. The apparent molecular weight of Swa$^{206-283}$ relative to globular protein standards (top chromatogram) is significantly higher in both states than its calculated mass, consistent with it being a nonglobular coiled-coil protein. To determine the dimerization constant, sedimentation velocity ultracentrifugation was performed at 20 °C. The calculated molecular mass obtained from the data is 17.1 kDa, which is between the molecular masses of Swa$^{206-283}$ monomer (11.7 kDa) and dimer (23.4 kDa),

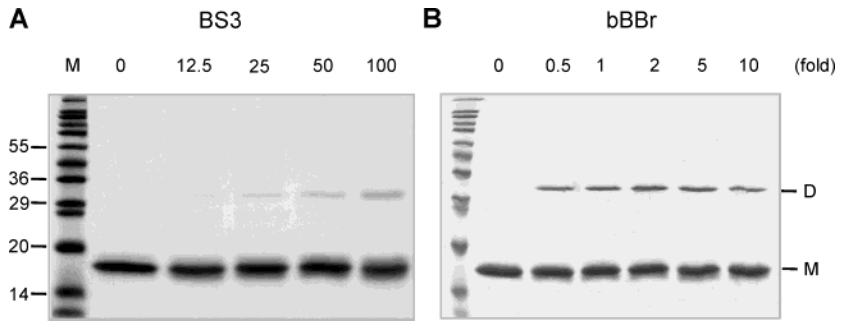

FIGURE 3: Chemical cross-linking with BS^3 and bBBr. (A) Cross-linking of Swa$^{191-297}$ with BS^3, which cross-links the ϵ-amine of lysine, is performed at a protein concentration of 5 μM in 50 mM sodium phosphate buffer, 0.5 M NaCl, and 10 mM β-mercaptoethanol, pH 6.0. The cross-linker was added at 12.5-, 25-, 50-, and 100-fold molar excess. (B) Cross-linking of Swa$^{206-283}$ with bBBr, a thiol-specific cross-linker, is performed at a protein concentration of 50 μM in 50 mM sodium phosphate buffer and 0.5 M NaCl, pH 6.0. The cross-linker was added at 0.5-, 1-, 2-, 5-, and 10-fold molar excess. The migration of monomer (M) and dimer (D) is slower than the molecular weight standards because of the high proportion of positively charged residues. The absence of higher molecular weight bands indicates that higher aggregates are not significantly populated.

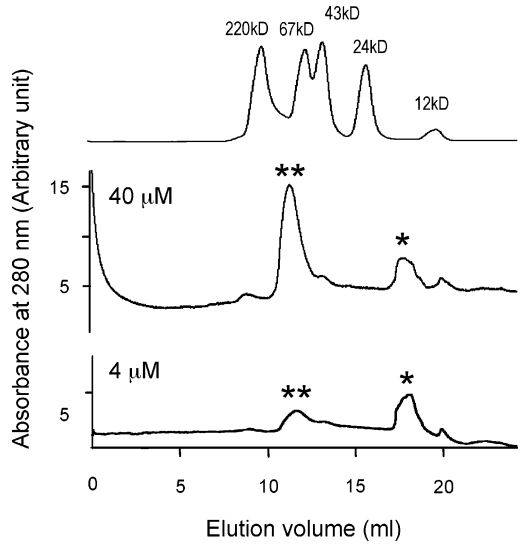

FIGURE 4: Size-exclusion chromatography of Swa$^{206-283}$. A Superdex 75 HR analytical column (Amersham Biosciences) was equilibrated with 50 mM sodium phosphate, pH 6, 0.4 M sodium sulfate, and 2 mM β-mercaptoethanol. Approximately 1 mL of Swa$^{206-283}$ at 4 or 40 μM was applied and eluted at 0.2 mL/min with the equilibration buffer at room temperature. Absorption at 280 nm is shown in arbitrary units. The low and high molecular weight peaks are indicated by * and **, respectively, and gave bands on SDS−PAGE consistent with the size of monomeric Swa$^{206-283}$ (data not shown). Topmost chromatogram shows elution volumes of globular protein standards.

indicating a monomer dimer equilibrium with a higher population of the monomer. The data were fit with the Sedanal software to a monomer−dimer equilibrium model with a dissociation constant of 4 μM, consistent with a weak dimeric coiled-coil.

Direct Interaction of Swallow Constructs with LC8 in Vitro. To test if swallow binds to LC8 directly, we performed GST pull-down assays using purified proteins. Figure 5A shows that LC8 binds efficiently to GST-Swa$^{191-297}$ but not to GST alone (lanes 2 and 3). Reverse GST pull-down assays show that Swa$^{206-297}$ interacts with GST-LC8 but not GST alone (Figure 5B, lanes 2 and 4). These two experiments confirm that the swallow domain including amino acids 206−297 direclty interacts with LC8. However, Swa$^{206-283}$, a truncated form lacking residues 284−297, shows only a residual level of interaction (Figure 5B, lane 5) suggesting that these residues are essential for mediating a strong interaction with LC8.

To map the LC8 binding site, limited tryptic digestion of Swa$^{191-297}$ in the presence and absence of LC8 (lanes marked + and − in Figure 6) were performed at an enzyme-to-substrate ratio of 1:50 (w/w). A large percentage of free Swa$^{191-297}$ was cleaved within 2 min, indicating a high susceptibility to tryptic digestion at room temperature. However, when an equimolar mixture of Swa$^{191-297}$ and LC8 was exposed to trypsin at the same enzyme-to-substrate ratio, the band for Swa$^{191-297}$ remained intact at 5 min and a significant proportion of it was uncleaved after 30 min of treatment (Figure 6). The above observation suggests that free Swa$^{191-297}$ is a relatively unstable protein, as expected for a weak dimeric coiled-coil, and LC8 binding increases its stability or average structure, making it less susceptible to proteolysis.

Fragments resulting from tryptic digestion of Swa$^{191-297}$ with and without LC8 were mapped by ESI-MS. Trypsin is a suitable enzyme for these experiments because Swa$^{191-297}$ contains a number of well-distributed trypsin-cutting sites (Figure 7). Table 1 lists the fragments of interest, their position in the sequence, and their intensities with and without LC8. Comparison of intensities of fragments 292−297, 188−297, and 286−297 with and without LC8 shows that Lys291 is protected in the presence of LC8, indicating that it lies within or adjacent to the Swa−LC8 interface. Fragment 292−297, formed by cleavage of Lys291, was mainly observed in the absence of LC8, while fragments 188−297 and 286−297 (which contain uncleaved Lys291) were observed only in the presence of LC8. In contrast, several arginine and lysine residues were equally accessible to trypsin both with and without LC8. For example, Arg285 and Arg208 (in fragments 188−285 and 188−208, respectively) are not protected in the presence of LC8, as indicated

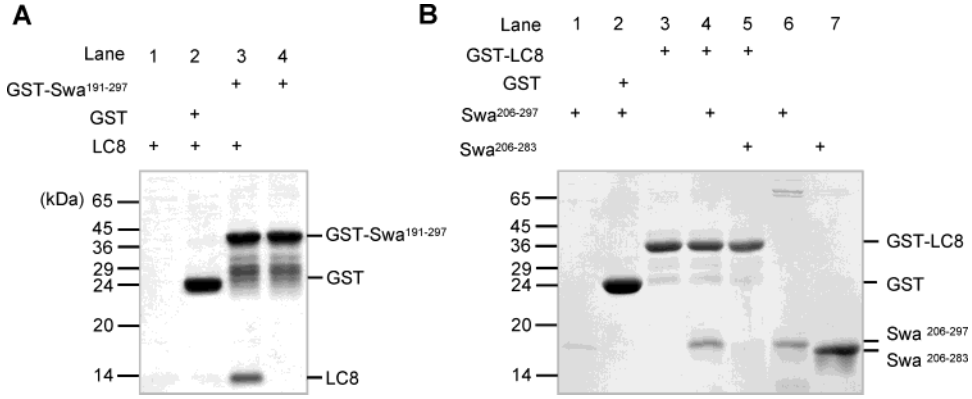

FIGURE 5: GST pull-down assays. (A) GST-Swa$^{191-297}$ is used for interaction with LC8. LC8 (lane 1), GST and LC8 (lane 2), and GST-Swa$^{191-297}$ and LC8 (lane 3) were mixed with glutathione−Sepharose 4B resins. For negative control, GST-Swa$^{191-297}$-conjugated resins were incubated with an equal volume of binding buffer instead of LC8 (lane 4). A band for LC8 appears only with GST-Swa$^{191-297}$, indicating specific binding (lane 3). (B) GST-LC8 is used for interaction with Swa$^{206-297}$. Swa$^{206-297}$ (lane 1), GST and Swa$^{206-297}$ (lane 2), and GST-LC8 and Swa$^{206-297}$ (lane 4) were incubated with the resin. For negative control, GST-LC8-conjugated resins were incubated with an equal volume of binding buffer instead of Swa$^{206-297}$ (lane 3). In lane 5, GST-LC8-conjugated resins were incubated with Swa$^{206-283}$. A band is present for Swa$^{206-297}$ (lane 4), indicating binding, while no band appears for Swa$^{206-283}$, indicating the absence of binding (lane 5). Lanes 6 and 7 show Swa$^{206-297}$ and Swa$^{206-283}$ loaded directly as markers ($^1/_{10}$ sample loading). The proteins that were bound to the resin were eluted by boiling in 2× sample loading buffer for 3 min, separated by SDS−15% PAGE, and stained with Coomassie brilliant blue.

Table 1: Preferential Cleavage Sites in Free Swa$^{191-297}$ and Swa$^{191-297}$−LC8 Complex Determined by Limited Tryptic Digestion

residues on Swa	sequences	calcd mass (kDa)	obsd mass (kDa)	intensity: Swa	intensity: Swa + LC8	residues protected
292−297	ATQTDF	682.3	682.5	9	1	K291
286−297	SATSAKATQTDF	1227.6	1227.6	2	10	K291
188−297	LTHSDSNYNSNSNNSSSSFDRLLAENESLQQKINSLRVEAKRLQGFNEY-VQERLDRKTDDFVKMKCNFETLRTELSECQQKLRRQQDNSQHHFMY-HIRSATSAKATQTDF	12 967.2	12 966.2	0	114	K291
188−228	LTHSDSNYNSNSNNSSSSFDRLLAENESLQQKINSLRVEAK	4599.9	4598.8	177	89	K228
188−285	LTHSDSNYNSNSNNSSSSFDRLLAENESLQQKINSLRVEAKRLQGFNEYV-QERLDRKTDDFVKMKCNFETLRTELSECQQKLRRQQDNSQHHFMYHIR	11 757.9	11 758.6	116	114	none
188−208	LTHSDSNYNSNSNNSSSSFDR	2332.9	2333.4	15	12	none
253−270	CNFETLRTELSECQQKLR	2197.9	2197.3	12	3	K252, R270

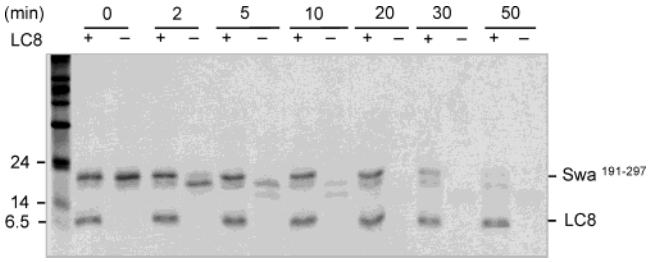

FIGURE 6: Limited tryptic digestion of Swa$^{191-297}$ in the free and LC8-bound states. SDS−PAGE shows 10 μM Swa$^{191-297}$ mixed with 1:1 molar ratio of LC8 (+) or equal volume of buffer for controls (−). Trypsin was added at an E:S (w/w) ratio of 1:50. Digestion was performed at 25 °C for 2, 5, 20, 30, and 50 min as indicated. Note that cleavage of LC8 is imperceptible under these conditions.

```
      191          201          211          221
RLTH SDSNYNSNSN NSSSSFDRLL AENESLQQKI NSLRVEAKRL
                                                 .....
231          241          251          261
QGFNEYVQER LDRKTDDFVK MKCNFETLRT ELSECQQKLR
.....................................................
271          281          291
RQQDNSQHHF MYHIRSATSA KATQTDF
.....                     ^
```

FIGURE 7: Primary amino acid sequence of Swa$^{191-297}$. The arginine and lysine residues are in boldface type, and those that are susceptible to trypsin as identified by mass spectrometry are underlined. The predicted α-helical coiled-coil region is indicated by the dotted line below the sequence. Residues before 191 were introduced by the expression tag and linker. K291, indicated by an arrow, is the site that is protected in the presence of LC8 (see Table 1).

by their similar intensities (Table 1). The specific protection of Lys291 suggests that the segment necessary for binding LC8 is downstream of Arg285 (since Arg285 is not protected), between residues 286 and 297. Note that this result is consistent with the absence of binding of Swa$^{206-283}$ to LC8 (Figure 5B, lane 5).

Another interesting observation in the comparison of fragment intensities is the protection in the presence of LC8 of the arginine and lysine residues within the predicted coiled-coil segment, underlined with a dotted line in Figure 7. For example, fragment 188−285, which is formed by cleavage at residues outside the predicted coiled-coil, is present in equal amounts with and without LC8, while fragment 188−228, which is formed by cleavage of Lys228 within the predicted coiled-coil, is half as intense in the presence of LC8. Fragment 253−270, with both cleavage sites within the predicted coiled-coil domain, is significantly less intense in the presence of LC8. We therefore conclude from these data obtained by limited proteolysis that there is protection both at the binding site and at sites distant from the interface, consistent with stabilization of the dimeric coiled-coil.

Increase in Stability of Swa$^{191-297}$ upon LC8 Binding. An increase in the stability of Swa$^{191-297}$ upon LC8 binding is manifested as an increase in resistance to thermal denaturation. Figure 8A shows thermal denaturation profiles at 222 nm of Swa$^{191-297}$ (●), LC8 (■), their linear summation (△), and their mixture (▲). As discussed earlier, free Swa$^{191-297}$ is a weak dimeric coiled-coil at 5 °C and undergoes reversible multistate unfolding with dissociation to a partially folded monomeric intermediate at 24 °C preceding complete unfolding at 50 °C (Figures 2 and 8, ●). In the presence of LC8 at a molar ratio of 2:1, a level baseline stable up to 35 °C replaces the first transition, and the thermal denaturation curve of Swa$^{191-297}$ appears to become two-state (Figure 8A, ▲). The ellipticity of LC8 at 222 nm (■) does not perceptibly change at temperatures below 65 °C, which is above the unfolding temperature of Swa$^{191-297}$. Since LC8 does not denature until after 65 °C, it is reasonable to assume that these changes in the CD signal at lower temperatures are a result of structural changes in Swa$^{191-297}$.

Figure 8B shows thermal unfolding profiles of Swa$^{206-283}$ in the presence and absence of LC8, performed similarly to the experiments with Swa$^{191-297}$ in Figure 8A. Swa$^{206-283}$ lacks the last 14 residues harboring the KATQT sequence and does not bind to LC8 (Figure 5B, lane 5). No appreciable difference is observed between the thermal unfolding profile of Swa$^{206-283}$ mixed with LC8 at a ratio of 1:4 (▲) and the linear summation of the profiles of Swa$^{206-283}$ and LC8 (△). This observation indicates that the change in thermal unfolding profile of Swa$^{191-297}$ observed upon LC8 binding is due to direct binding and not to molecular crowding.

To determine whether LC8 binding is specific, we performed several thermal denaturation experiments at a constant concentration of Swa$^{191-297}$ and increasing concentration of LC8. Figure 9 shows the percentage increase in stabilization of Swa$^{191-297}$ at increasing LC8 concentration. The increase in stabilization of the first transition was measured as the percentage of increase in negative ellipticity at 222 nm at 29 °C, the temperature at which the difference in negative ellipticity between the sum and mix is the largest (Figure 8A). The data show that stabilization of the coiled-coil domain of swallow is concentration-dependent at lower LC8 concentrations and reaches saturation at a molar ratio of LC8 to Swa$^{191-297}$ greater than 1:1.

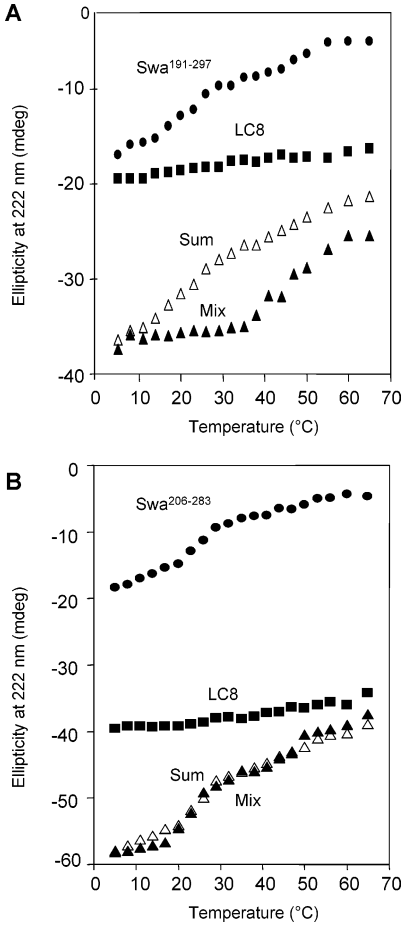

FIGURE 8: Effect of LC8 binding on stability of Swa$^{191-297}$. (A) Thermal denaturation curves of Swa$^{191-297}$ (●), LC8 (■), their computed sum (△), and a 1:2 mixture of Swa$^{191-297}$ and LC8 (▲) are shown. The computed sum represents the hypothetical curve if there is no interaction between the two proteins. The concentrations of Swa$^{191-297}$ and LC8 were 1.5 and 3 μM, respectively. In the presence of LC8, the first transition is replaced with a stable baseline. (B) Thermal denaturation curves of Swa$^{206-283}$ (●), LC8 (■), their computed sum (△), and a 1:4 mixture of Swa$^{206-283}$ and LC8 (▲) are shown. The concentrations of Swa$^{206-283}$ and LC8 were 1.5 and 6 μM, respectively. The overlay of the mixture and sum curves indicates that there is no interaction between Swa$^{206-283}$ and LC8 and that the increase in stability of Swa$^{191-297}$ is interaction-dependent, not simply due to molecular crowding.

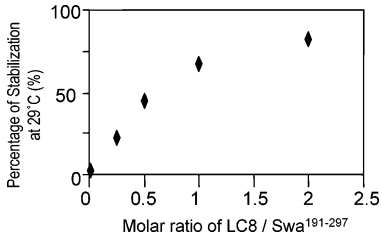

FIGURE 9: Protein concentration dependence of the LC8−swallow interaction. Percentage of stabilization of Swa$^{191-297}$ at 29 °C is plotted as a function of increasing molar ratio of LC8 to Swa$^{191-297}$. For each concentration, a complete thermal unfolding curve was obtained (data not shown). The percentage of stabilization was calculated from $[\theta_{222}(29\ °C)_i - \theta_{222}(29\ °C)_0]/\theta_{222}(5\ °C)_0$, where i stands for the molar ratio of LC8 to Swa$^{191-297}$, $\theta_{222}(29\ °C)_i$ represents the ellipticity of the mixture of Swa$^{191-297}$ and LC8 at 29 °C, and $\theta_{222}(29\ °C)_0$ and $\theta_{222}(5\ °C)_0$ are ellipticities of free Swa$^{191-297}$ at 29 and 5 °C, respectively. The saturation of binding observed is further indication of specific binding.

Increase in the Population of Dimeric Coiled-Coil of Swa$^{191-297}$ upon LC8 Binding. Chemical cross-linking of

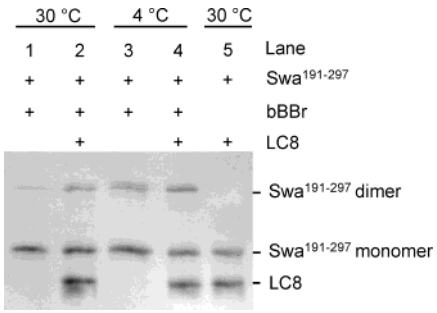

FIGURE 10: Covalent cross-linking of Swa$^{191-297}$ in the presence and absence of LC8 at 4 and 30 °C. Swa$^{191-297}$ at a concentration of 5 μM was preincubated with an equal concentration of LC8 in 50 mM sodium phosphate, 0.5 M NaCl, and 1 mM TCEP, pH 6.5, at 4 or 30 °C for 1 h. The thiol-specific cross-linker bBBr was added to a final concentration of 200 μM. Lanes 1 and 2 correspond to Swa$^{191-297}$ in the absence and presence of LC8 at 30 °C, and lanes 3 and 4 correspond to Swa$^{191-297}$ in the absence and presence of LC8 at 4 °C. Lane 5 shows Swa$^{191-297}$ and LC8 at 30 °C in the absence of the cross-linker. There is no perceptible difference in the intensity of the bands corresponding to the dimer with and without LC8 at 4 °C, but there is a significant increase in intensity of the dimer band in the presence of LC8 at 30 °C, indicating that LC8 promotes dimer formation at 30 °C, while at 4 °C, Swa$^{191-297}$ is primarily dimeric.

Swa$^{191-297}$ was performed at 4 and 30 °C in the presence and absence of LC8 to determine the effect of temperature and LC8 binding on the population of the dimeric coiled-coil (Figure 10). Since bBBr, a zero-length cross-linker, was used, an increase in the cross-linked product was explained to result from an increase in the population of the dimer, rather than structural rearrangements of the reactive residues at different temperatures or their enforced proximity upon binding to dimeric LC8. At 4 °C, there is no significant difference in the extent of cross-linking of Swa$^{191-297}$ in the presence and absence of LC8, indicating that at this temperature the dimer is equally populated at both conditions (Figure 10, lanes 3 and 4). At 30 °C, only a residual amount of Swa$^{191-297}$ was cross-linked in the absence of LC8 (Figure 10, lane 1), while in the presence of an equal concentration of LC8, a significant proportion of Swa$^{191-297}$ was cross-linked (Figure 10, lane 2). The increase in intensity of the band at 30 °C shows that the dimer is significantly more populated in the presence of LC8. Without LC8, Swa$^{191-297}$ does not cross-link at 30 °C even at higher concentration (data not shown), consistent with the loss of coiled-coil structure at elevated temperature, and further confirming that the stabilization of Swa$^{191-29}$ is not a result of nonspecific molecular crowding. Taken together, these observations verify that LC8 binding stabilizes Swa$^{191-297}$ coiled-coil dimer at higher temperature.

DISCUSSION

Direct Interaction between LC8 and Swallow Constructs. As a subunit of cytoplasmic dynein and myosin, LC8 is believed to act as an adapter or linker molecule that recruits and/or tethers various cargoes to the motors for transport (*32*). Among the putative dynein cargoes in *Drosophila* is the *bicoid* morphogen, an RNA-containing complex that establishes the anterior−posterior axis in *Drosophila*. The swallow gene product may link the *bicoid* RNA to LC8 and the dynein motor complex. A domain of swallow, Swa$^{191-297}$, has been identified by yeast two-hybrid assays to be sufficient

for binding LC8. Here we use GST pull-down assays (Figure 5) to show that this coiled-coil domain of swallow also binds tightly to LC8 in vitro. Binding was also monitored by protection from tryptic digestion (Figure 6 and Table 1) and an increase in negative ellipticity at 222 nm in CD spectra (Figure 8A). Residues 284−297 on swallow are sufficient for mediating a tight interaction with LC8. $Swa^{206-283}$, a truncated form that lacks amino acids 284−297, displays residual levels of interaction with LC8 in GST pull-down assays. In summary, in addition to verifying binding and mapping interaction sites, our results demonstrate that LC8 binding causes substantial changes in the stability and quaternary structure of swallow.

Swallow Constructs Form a Weak Dimeric Coiled-Coil. An array of experiments were used to characterize the structure and the association state of the recombinant swallow constructs. The evidence that the swallow constructs form a dimeric coiled-coil consistent with Multicoil prediction comes from the following: CD spectra are typical of an α-helix, with double minima at 208 and 222 nm, and the $[\theta_{222}]/[\theta_{208}]$ ratio is greater than 1, indicating supercoiling (Figure 2A). Size-exclusion chromatography reveals two molecular states whose populations are concentration-dependent, and elution times are indicative of nonglobular proteins (Figure 4). Chemical cross-linking demonstrates that the swallow construct is primarily monomeric at 30 °C and dimeric at 4 °C, with a cysteine residue at the interface and a lysine residue close to the interface (Figures 3 and 10). Sedimentation velocity gives a dissociation constant of 4 μM at 20 °C, consistent with a weak dimer.

Dimeric coiled-coils most commonly unfold in a single two-state transition and at considerably higher temperatures than those observed for the swallow coiled-coil domain (*31*, *33*). The swallow coiled-coil domain unfolds in an apparent three-state mechanism, showing protein concentration dependence only during the first transition (Figure 2B). The concentration-dependent first transition is due to a loss of supercoiling and subsequent dimer dissociation. The unimolecular second transition reflects unfolding of the remaining helical structure. It is our contention that the instability of the swallow constructs relative to other coiled-coil proteins is a characteristic of native swallow and is not due to truncation of the folding domain. Coiled-coils are generally independently folded domains, and we have included in our constructs the entire domain as predicted by Multicoil. Also, we do not observe greater stability in the longer constructs.

Comparison of the swallow sequence to coiled-coil model peptides suggests reasons for its instability. A typical stable parallel dimeric coiled-coil has several β-branched residues, valine or isoleucine, in the a position and leucine residues in the d position (*34*). In swallow, there is only one isoleucine in the a position and five leucine residues in the d position of the 10-heptad coiled-coil (Figure 1B). The typical coiled-coil is further stabilized by salt bridges between residues in the g (*i*) and e′ ($i + 5$) positions (*30*, *34*). Swallow has a single stabilizing salt bridge between Asp247 and Lys252 and has a destabilizing interaction between Lys219 and Arg224 (Figure 1B). This inherent instability of the swallow coiled-coil allows it to exist as a monomer or dimer in vivo, with its association state being environment-dependent. Transient dimers are common in signaling pathways, regulation, and DNA binding proteins (*35*), where monomers and dimers have separate functions.

LC8 Binding Increases the Stability of the Dimeric Coiled-Coil. Several experiments verify that LC8 binding stabilizes the coiled-coil dimer of swallow. Limited proteolysis of the swallow coiled-coil domain in the presence of an equimolar ratio of LC8 shows a significant increase in resistance to tryptic digestion at sites distant from binding. Tryptic fragments identified by mass spectrometry show protection of arginine and lysine residues within the coiled-coil domain in the presence of LC8 in addition to protection at the binding site (Table 1). Resistance to proteolysis could be due to an increase in protein stability or to a structural change or both (*36*).

Thermal denaturation experiments monitored by CD at 222 nm and covalent cross-linking as a function of temperature verify that LC8 binding favors the dimerization of the coiled-coil domain of swallow that is otherwise primarily monomeric at room temperature. The thermal unfolding profile of free $Swa^{191-297}$ was compared to that of LC8−$Swa^{191-297}$ mixture (Figure 8A). In the presence of LC8, $Swa^{191-297}$ primarily exists as a dimeric coiled-coil and does not begin to dissociate till after 35 °C. The dimerization coupled to LC8 binding was confirmed by cross-linking experiments (Figure 10). At 30 °C, the temperature at which free $Swa^{191-297}$ is primarily monomeric, there is no detectable cross-linking, but in the presence of LC8 a significant increase in cross-linking is observed, indicating that LC8 binding increases the population of the dimer. At 4 °C, the difference is not as noticeable, indicating that the coiled-coil dimer is already significantly populated before binding. Our explanation of these results is that LC8 binding is essential for the assembly of the dimeric coiled-coil in the physiological temperature range of 25−35 °C, while free swallow is primarily monomeric in this temperature range.

Functional Implications. The observation that LC8 binding mediates the assembly of swallow domain into a stable coiled-coil raises several intriguing questions. Why is swallow a weak dimeric coiled-coil that becomes tighter upon binding to LC8? Is there a role for this transient dimer in the function of the swallow protein? We speculate that, upon binding to LC8, the stabilized coiled-coil domain may in turn facilitate the binding of swallow to other macromolecules. Immediately upstream of the coiled-coil domain is a positively charged region that bears significant homology to a double-stranded RNA (dsRNA) recognition motif (Figure 1A). Formation of a tight dimer upon LC8 binding may increase the binding affinity of swallow to the putative dsRNA. This mechanism could function to regulate the proposed binding and anterior transport of *bicoid* mRNA by dynein (*13*). Our work does not establish that LC8 links swallow to the native dynein motor complex, and further work is necessary. Alternatively, *bicoid* mRNA may be prelocalized and the subsequent LC8 binding to swallow may establish the stable anchoring of *bicoid* mRNA at the oocyte anterior (*37*). In this regard, formation of a coiled-coil of swallow is similar to the formation of the cJun and cFos heterodimer coiled-coil, which is required for proper alignment of the DNA recognition domains (*38*).

Coiled-coil domains are known to act as molecular recognition motifs. Recent examples include laminin (*39*), the actin-binding protein coronin (*40*), and the silent infor-

mation regulator Sir4 (*41*). In the coiled-coil domain of yeast Sir4, for example, residues from both chains of the coiled-coil form the interaction surface with Sir3, which in turn assists the spreading and maintenance of silent DNA (*41*). The Sir3 interaction with both subunits of the coiled-coil of Sir4 indicates that the stability of the dimeric coiled-coil is necessary for this interaction. It is possible that the dimeric coiled-coil of swallow is a recognition motif for other molecules that are recruited to the complex only upon LC8 binding.

The stabilization of swallow upon LC8 binding supports the view that LC8 is a promoter of macromolecular assembly and stabilization in multiple situations both within and outside the dynein complex. Within the dynein complex, LC8 may initiate complex assembly by promoting an increase in structure and stability of dynein intermediate chains. This proposal is based on in vitro studies with recombinant N-terminal domain of IC74 and LC8 (*21*, *42*). Upon LC8 binding, the primarily unstructured IC74 domain becomes more resistant to protease digestion and shows an increase in CD-detected α-helical or coiled-coil structure. Genetic experiments on filamentous fungi also suggest that LC8 is important in providing thermodynamic stability to the dynein complex. Liu et al. (*43*) created a deletion mutation at the *nudG* gene that encodes the LC8 analogue of the filamentous fungus *Aspergillus nidulans.* Interestingly, colonies grown at 23 °C are completely normal, whereas colonies grown at 42 °C acquire defects that phenocopy the NudA or the dynein heavy-chain null mutants. This experiment suggests that, in some organisms, the primary function of LC8 is to prevent dissociation of the dynein complex at elevated temperature. Here, we provide evidence that LC8 binds the swallow protein and promotes its assembly into a dimeric coiled-coil that is a partially folded monomer in the absence of LC8 in the physiological temperature range. In this regard, LC8 appears to have a role not only limited to the assembly of dynein complex or cargo recognition but also in folding and assembly of complexes outside of dynein.

REFERENCES

1. King, S. M., and Patel-King, R. S. (1995) The M(r) = 8,000 and 11,000 outer arm dynein light chains from *Chlamydomonas* flagella have cytoplasmic homologues, *J. Biol. Chem. 270*, 11445−52.
2. King, S. M. (2000) The dynein microtubule motor, *Biochim. Biophys. Acta*−*Mol. Cell Res. 1496*, 60−75.
3. Dick, T., Ray, K., Salz, H. K., and Chia, W. (1996) Cytoplasmic dynein (ddlc1) mutations cause morphogenetic defects and apoptotic cell death in *Drosophila melanogaster*, *Mol. Cell Biol. 16*, 1966−77.
4. Beckwith, S. M., Roghi, C. H., Liu, B., and Ronald Morris, N. (1998) The "8-kD" cytoplasmic dynein light chain is required for nuclear migration and for dynein heavy chain localization in *Aspergillus nidulans*, *J. Cell Biol. 143*, 1239−47.
5. Pazour, G. J., Wilkerson, C. G., and Witman, G. B. (1998) A dynein light chain is essential for the retrograde particle movement of intraflagellar transport (IFT), *J. Cell Biol. 141*, 979−92.
6. Phillis, R., Statton, D., Caruccio, P., and Murphey, R. K. (1996) Mutations in the 8 kDa dynein light chain gene disrupt sensory axon projections in the *Drosophila* imaginal CNS, *Development 122*, 2955−63.
7. McGrail, M., and Hays, T. S. (1997) The Microtubule Motor Cytoplasmic Dynein Is Required For Spindle Orientation During Germline Cell Divisions and Oocyte Differentiation In *Drosophila*, *Development 124*, 2409−2419.
8. King, S. M., Barbarese, E., Dillman, J. F., 3rd, Benashski, S. E., Do, K. T., Patel-King, R. S., and Pfister, K. K. (1998) Cytoplasmic dynein contains a family of differentially expressed light chains, *Biochemistry 37*, 15033−41.
9. Espindola, F. S., Suter, D. M., Partata, L. B. E., Cao, T., Wolenski, J. S., Cheney, R. E., King, S. M., and Mooseker, M. S. (2000) The light chain composition of chicken brain myosin-Va: Calmodulin, myosin-II essential light chains, and 8-kDa dynein light chain/PIN, *Cell Motil. Cytoskeleton 47*, 269−281.
10. Benashski, S. E., Harrison, A., Patel-King, R. S., and King, S. M. (1997) Dimerization of the highly conserved light chain shared by dynein and myosin V, *J. Biol. Chem. 272*, 20929−35.
11. Kaiser, F. J., Tavassoli, K., Van Den Bemd, G. J., Chang, G. T., Horsthemke, B., Moroy, T., and Ludecke, H. J. (2003) Nuclear interaction of the dynein light chain LC8a with the TRPS1 transcription factor suppresses the transcriptional repression activity of TRPS1, *Hum. Mol. Genet. 12*, 1349−58.
12. Puthalakath, H., Huang, D. C. S., O'Reilly, L. A., King, S. M., and Strasser, A. (1999) The proapoptotic activity of the Bcl-2 family member Bim is regulated by interaction with the dynein motor complex, *Mol. Cell 3*, 287−296.
13. Schnorrer, F., Bohmann, K., and Nusslein-Volhard, C. (2000) The molecular motor dynein is involved in targeting swallow and bicoid RNA to the anterior pole of *Drosophila* oocytes, *Nat. Cell Biol. 2*, 185−90.
14. Jaffrey, S. R., and Snyder, S. H. (1996) PIN: An associated protein inhibitor of neuronal nitric oxide synthase, *Science 274*, 774.
15. Naisbitt, S., Valtschanoff, J., Allison, D. W., Sala, C., Kim, E., Craig, A. M., Weinberg, R. J., and Sheng, M. (2000) Interaction of the postsynaptic density-95/guanylate kinase domain-associated protein complex with a light chain of myosin-V and dynein, *J. Neurosci. 20*, 4524−34.
16. Fuhrmann, J. C., Kins, S., Rostaing, P., El Far, O., Kirsch, J., Sheng, M., Triller, A., Betz, H., and Kneussel, M. (2002) Gephyrin interacts with Dynein light chains 1 and 2, components of motor protein complexes, *J. Neurosci. 22*, 5393−402.
17. Raux, H., Flamand, A., and Blondel, D. (2000) Interaction of the rabies virus P protein with the LC8 dynein light chain, *J. Virol. 74*, 10212−10216.
18. Jacob, Y., Badrane, H., Ceccaldi, P. E., and Tordo, N. (2000) Cytoplasmic dynein LC8 interacts with lyssavirus phosphoprotein, *J. Virol. 74*, 10217−10222.
19. St. Johnston, D., Driever, W., Berleth, T., Richstein, S., and Nusslein-Volhard, C. (1989) Multiple steps in the localization of bicoid RNA to the anterior pole of the Drosophila oocyte, *Development 107* (suppl.), 13−19.
20. Berleth, T., Burri, M., Thoma, G., Bopp, D., Richstein, S., Frigerio, G., Noll, M., and Nusslein-Volhard, C. (1988) The role of localization of bicoid RNA in organizing the anterior pattern of the *Drosophila* embryo, *EMBO J. 7*, 1749−56.
21. Makokha, M., Hare, M., Li, M., Hays, T., and Barbar, E. (2002) Interactions of cytoplasmic dynein light chains Tctex-1 and LC8 with the intermediate chain IC74, *Biochemistry 41*, 4302−11.
22. Barbar, E., Kleinman, B., Imhoff, D., Li, M., Hays, T. S., and Hare, M. (2001) Dimerization and folding of LC8, a highly conserved light chain of cytoplasmic dynein, *Biochemistry 40*, 1596−605.
23. Rohl, C. A., and Baldwin, R. L. (1997) Comparison of NH exchange and circular dichroism as techniques for measuring the parameters of the helix−coil transition in peptides, *Biochemistry 36*, 8435−42.
24. Stafford, W. F., 3rd (1992) Boundary analysis in sedimentation transport experiments: a procedure for obtaining sedimentation coefficient distributions using the time derivative of the concentration profile, *Anal. Biochem. 203*, 295−301.
25. Lupas, A., Van Dyke, M., and Stock, J. (1991) Predicting coiled-coils from protein sequences, *Science 252*, 1162−4.
26. Wolf, E., Kim, P. S., and Berger, B. (1997) MultiCoil: a program for predicting two- and three-stranded coiled-coils, *Protein Sci. 6*, 1179−89.
27. Jones, D. T. (1999) Protein secondary structure prediction based on position-specific scoring matrices, *J. Mol. Biol. 292*, 195−202.
28. Rodriguez-Crespo, I., Yelamos, B., Roncal, F., Albar, J. P., Ortiz de Montellano, P. R., and Gavilanes, F. (2001) Identification of novel cellular proteins that bind to the LC8 dynein light chain using a pepscan technique, *FEBS Lett. 503*, 135−41.

29. Muhle-Goll, C., Gibson, T., Schuck, P., Schubert, D., Nalis, D., Nilges, M., and Pastore, A. (1994) The dimerization stability of the HLH-LZ transcription protein family is modulated by the leucine zippers: a CD and NMR study of TFEB and c-Myc, *Biochemistry 33*, 11296−306.
30. Zhou, N. E., Kay, C. M., and Hodges, R. S. (1994) The role of interhelical ionic interactions in controlling protein folding and stability. De novo designed synthetic two-stranded alpha-helical coiled-coils, *J. Mol. Biol. 237*, 500−12.
31. Dutta, K., Alexandrov, A., Huang, H., and Pascal, S. M. (2001) pH-induced folding of an apoptotic coiled-coil, *Protein Sci. 10*, 2531−40.
32. Hays, T., and Karess, R. (2000) Swallowing dynein: a missing link in RNA localization? *Nat. Cell Biol. 2*, E60−2.
33. Sosnick, T. R., Jackson, S., Wilk, R. R., Englander, S. W., and DeGrado, W. F. (1996) The role of helix formation in the folding of a fully alpha-helical coiled-coil, *Proteins: Struct., Funct., Genet. 24*, 427−32.
34. Acharya, A., Ruvinov, S. B., Gal, J., Moll, J. R., and Vinson, C. (2002) A heterodimerizing leucine zipper coiled-coil system for examining the specificity of a position interactions: amino acids I, V, L, N, A, and K, *Biochemistry 41*, 14122−31.
35. Nooren, I. M. A., and Thornton, J. M. (2003) Structural characterisation and functional significance of transient protein−protein interactions, *J. Mol. Biol. 325*, 991−1018.
36. Carey, J. (2000) in *Applications of Chimeric Genes and Hybrid Proteins, Pt C* (Thorner, J. E., and Abelson, S. D., Eds.) Academic Press, San Diego, CA.
37. Palacios, I. M., and St. Johnston, D. (2001) Getting the message across: The intracellular localization of mRNAs in higher eukaryotes, *Annu. Rev. Cell Dev. Biol. 17*, 569−614.
38. Kouzarides, T., and Ziff, E. (1989) Leucine zippers of fos, jun and GCN4 dictate dimerization specificity and thereby control DNA binding, *Nature 340*, 568−71.
39. Sanz, L., Garcia-Bermejo, L., Blanco, F. J., Kristensen, P., Feijoo, M., Suarez, E., Blanco, B., and Alvarez-Vallina, L. (2003) A novel cell binding site in the coiled-coil domain of laminin involved in capillary morphogenesis, *EMBO J. 22*, 1508−17.
40. Humphries, C. L., Balcer, H. I., D'Agostino, J. L., Winsor, B., Drubin, D. G., Barnes, G., Andrews, B. J., and Goode, B. L. (2002) Direct regulation of Arp2/3 complex activity and function by the actin binding protein coronin, *J. Cell Biol. 159*, 993−1004.
41. Chang, J. F., Hall, B. E., Tanny, J. C., Moazed, D., Filman, D., and Ellenberger, T. (2003) Structure of the coiled-coil dimerization motif of Sir4 and its interaction with Sir3, *Structure 11*, 637−49.
42. Nyarko, A., Makokha, M., M., H., and Barbar, E. (2003) Interactions of LC8 with N-terminal Segments of the Intermediate Chain of Cytoplasmic Dynein, *Sci. World J. 3*, 647−654.
43. Liu, B., Xiang, X., and Lee, Y. R. (2003) The requirement of the LC8 dynein light chain for nuclear migration and septum positioning is temperature dependent in *Aspergillus nidulans*, *Mol. Microbiol. 47*, 291−301.

BI036328X